Intern. J. Fuzzy Mathematical Archive
Vol. 22, No. 1, 2024, 15-32
ISSN: 2320 –3242 (P), 2320 –3250 (online)
Published on 7 July 2024
www.researchmathsci.org
DOI: http://dx.doi.org/10.22457/ijfma.v22n1a02241

International Journal of Fuzzy Mathematical Archive

Fuzzy Logic Analysis of the Effects of Eckert Number on Casson Micropolar Nanofluid Flow over an Inclined Magnetic Field with Chemical Reactions

N.Ramya [1], ***M. Deivanayaki**** [2] **and** ***Farshid Mofidnakhaei*** [3]

[1]Research Scholar, Karpagam Academy of Higher Education, Coimbatore, India
E-mail: jpramyamaths@gmail.com
[2]Associate Professor, Department of Science and Humanities,
Karpagam Academy of Higher Education, Coimbatore, India
[3]Department of Physics, Sari Branch, Islamic Azad University, Sari, Iran.
E-mail:farshid.mofidnakhaei@gmail.com
*Corresponding author.

Received 2 June 2024; accepted 6 July 2024

Abstract. Fuzzy logic to investigate the effects of the Eckert number and chemical reactions on the flow characteristics of a Casson micropolar nanofluid under an inclined magnetic field. The system of partial differential equations describing the fluid dynamics is converted into ordinary differential equations with the aid of fuzzy logic techniques, and solved numerically using MATLAB’s bvp4c method. Graphical analysis illustrates how variations in the Eckert number impact the velocity, magnetic field, micropolar properties, temperature, and concentration profiles. Results indicate that an increase in the Eckert number decreases fluid concentration while inversely affecting the temperature profile.

Keywords: Stretching sheet, Lorentz force, Eckert number, Magnetic field, Micropolar.

AMS Mathematics Subject Classification (2010): 90B05

1. Introduction

In recent years, the exploration of nanofluid dynamics has significantly increased owing to its essential roles in diverse engineering and industrial applications, including heat exchangers, biomedical devices, and solar collectors. Casson micropolar nanofluids, noted for their non-Newtonian properties and capability to integrate micro-rotational effects, present distinctive benefits in improving the efficiency of heat and mass transfer processes. Electro magnetohydrodynamics with the Casson nanofluid across the permeable Riga surface are impacted by biological processes [1,2]. The thermal characteristics of a ternary nano liquid formed of water and including metallic and oxide nanoparticles (MoS2, SiO2, and Au) while it navigates an annulus that is exposed to thermal expansion creatures, coupled transpiration, frictional warmth, and a typical field of magnets [3]. Computational exploration is done for the unstable magnetohydrodynamic (MHD) frontier layer slip movement and heat transfer of tiny fluids in a solar collector, which is possibly modelled as a regressive extending sheet [4]. The role on warmth emission and intake on the magnetohydrodynamic boundary-layer flow of Casson nanofluid across a non-linear extending material in two aspects, along with the dissipated [5-8]. The ramifications of ultraviolet light on a two-dimensional tiny fluid's stagnation-point movement across an expanding sheet were examined [9]. Numerous enzyme activities, including the transit of objects, diagnostic surgeries, the supply of circulating blood from the coronary arteries to different areas of the physique, and the regulation of warmth travel things, depend heavily on periodic slips are discussed [10-12]. Comprehensive research can be done on the repercussions of ultraviolet (UV) thermal movement and slip state on dispersion in relation to Casson nanofluid movement analyzed [13, 14]. The discussion focuses on the bilateral process triggered by Arrhenius activating in the hydromagnetic stagnation point flow of Casson nanofluid across an extensible sheet in a non-Darcy porous substance [15]. How warmth, viscosity disuse, and the biological processes modify Williamson nanofluid's sticking limit movement across an exponentially expanding sheet discussed [16, 17]. In an environment of bulk evaporation and process, constant magnetohydrodynamics (MHD) incompressible hybrid nanofluid flow and conveyance of mass caused by permeable extending surface with quadratic pace are studied [18]. The mass and warmth transfer in thermophoretic warming hydromagnetic nanofluid movement over a substantially expanding permeable sheet encased in a medium that is permeable, taking into account the ramifications of vacuum, infusion, and viscous dissipation in addition to warmth production and adsorption are examined [19]. The magnetohydrodynamic nanofluid flow via a permeable linear extensible sheet while it is subjected to warming by convection and a matrix with permeability discussed [20-24,46]. The constrained movement of fluid patterns is fascinating to study owing to its role in several commercial uses discussed [25-32]. The concepts of vertex regularity within cubic fuzzy graph structures and applies these concepts to practical problems are discussed [34,45]. The properties of interval-valued quadri partitioned neutrosophic graphs and demonstrate their application in real-life scenarios, domination in vague graphs, complex Pythagorean fuzzy graphs, energies of picture fuzzy graphs, transferring cancer patients between countries and fully connected cubic networks explored [35-44].

Conventional analytical and numerical techniques frequently encounter challenges due to the inherent complexities and nonlinear behaviors of such systems, particularly when multiple parameters interact in unpredictable ways. Fuzzy logic offers a powerful framework for addressing uncertainties and modeling intricate relationships within fluid dynamics. By integrating fuzzy logic into the analysis, it becomes feasible to manage uncertainties more effectively and derive approximate solutions for systems where precise solutions are challenging to obtain or computationally prohibitive. This study aims to apply fuzzy logic to examine the impact of the Eckert number on the flow and thermal properties of a Casson micropolar nanofluid in the context of chemical reactions and an inclined magnetic field. The specific objectives include:

- Developing a fuzzy logic-based methodology to convert the governing partial differential equations (PDEs) into ordinary differential equations (ODEs).
- Exploring how variations in the Eckert number affect the velocity, temperature, and concentration profiles.
- Offering a comparative analysis of the findings with and without the application of fuzzy logic to demonstrate the benefits of this approach.

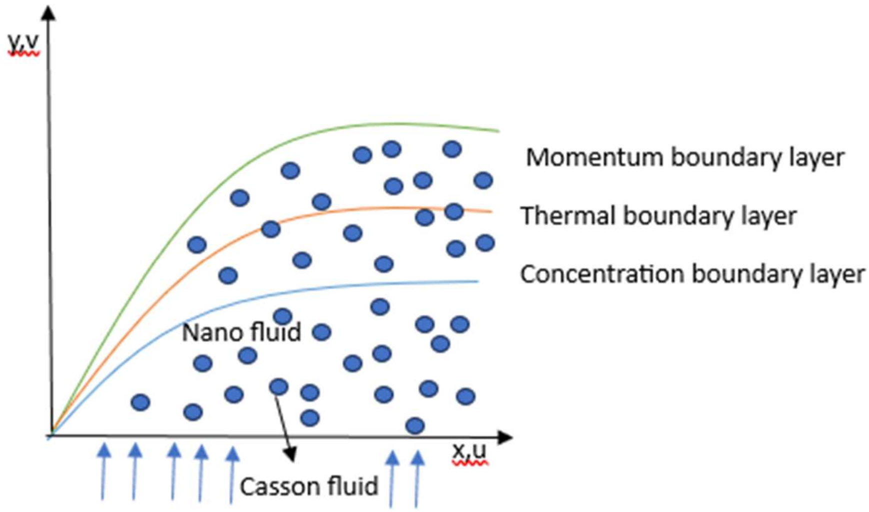

Fig 1:

Nomenclature

(u,v)	Velocity components	q'''	Irregular heat parameter	M	Hartmann number
β_T	Thermal coefficient	D_m	Mass diffusivity	N_r	Radiative parameter
β_c	Concentration coefficient	C_s	Concentration susceptibility	S_r	Soret number
T	Fluid temperature	K_T	Thermal diffusion ratio	S_C	Schmidt number
T_∞	Uniform temperature	T_m	Mean temperature	D_u	Dufour number
C	Concentration fluid	B_{iT}	Thermal Biot Number	E_c	Eckert number
C_∞	Uniform concentration	B_{iC}	Mass Biot Number	K_r	Chemical parameter
α	Angle of inclination	Υ	Velocity slip parameter	q_r	Radiative heat
σ	Electric conductivity fluid	G_{rT}	Thermal Grashot number	K	Non dimensional parameter
B_0	Uniform magnetic field			P_r	Prandtl number
g	Gravitational acceleration			G_{rc}	Solutal Grashot number

2. Mathematical analysis

The analysis of Casson micropolar nanofluid flow over an inclined magnetic field with chemical reactions, the sustainability equations for continuity, momentum, and energy are presented as follows

Continuity equation

The continuity equation ensures mass conservation in the fluid flow and is given by

$$\frac{\partial u}{\partial x} + \frac{\partial u}{\partial y} = 0$$

Momentum equation

For Casson micropolar nanofluids, the momentum equation accounts for both Newtonian and non-Newtonian effects along with magnetic field influence. It can be written as

$$u\frac{\partial u}{\partial x}+v\frac{\partial u}{\partial y}=\nu\left(1+\frac{1}{\beta}\right)\left(\frac{\partial^2 u}{\partial y^2}\right)-\left(\frac{k_1}{\rho}\right)\frac{\partial N}{\partial y}+[g\beta_T(T-T_\infty)\cos\alpha+g\beta_C(C-C_\infty)]\cos\alpha-\frac{\sigma B_0^2\,u}{\rho}---(1)$$

Microrotation equation

The microrotation equation describes the behavior of microrotation within the fluid, considering both rotational viscosity and the applied magnetic field effects. The equation is

$$u\frac{\partial N}{\partial x}+v\frac{\partial N}{\partial y}=\frac{\gamma}{\rho}\frac{\partial^2 N}{\partial y^2}-\left(\frac{k_1}{\rho}\right)\left(1+\frac{1}{\beta}\right)\left(2N+\frac{\partial u}{\partial y}\right)---(2)$$

Energy equation

The energy equation, accounting for heat transfer and the effects of Eckert number and chemical reactions, is given by

$$\rho C_p\left[u\frac{\partial T}{\partial x}+v\frac{\partial T}{\partial y}\right]=k\frac{\partial^2 T}{\partial y^2}-\frac{\partial q_r}{\partial y}+q'''+\nu\rho\left[\frac{\partial u}{\partial y}\right]^2+\frac{\rho D_m k_T}{C_s}\frac{\partial^2 C}{\partial y^2}\quad--------(3)$$

Concentration equation

The concentration equation governs the distribution of species within the fluid and incorporates effects like diffusion and chemical reactions. It can be expressed as

$$u\frac{\partial C}{\partial x}+v\frac{\partial C}{\partial y}=D_m\frac{\partial^2 C}{\partial y^2}-k^*(C-C_\infty)+\frac{D_m k_T}{T_m}\frac{\partial^2 T}{\partial y^2}-----(4)$$

The irregular heat parameter is defined by

$$q'''=\frac{ku_w}{x\upsilon}\left(A^*(T_w-T_\infty)f'+B^*(T-T_\infty)\right)----(5)$$

The temperature difference between T and the free surge temperature T_∞ is tiny, and by removing components of higher order, Taylor's simplification concerning T_∞ is $T_w=T_\infty+bx$. The following equation is the result of using Rosland's approximation for thermal radiation.

$$q_r=-\frac{16}{3}\frac{\sigma^*}{k^*}T^3\frac{\partial T}{\partial y}\quad----(6)$$

The boundary conditions as

$$u=u_w+L\left[\frac{\partial u}{\partial y}\right],-k\left[\frac{\partial T}{\partial y}\right]=h_1[T_\infty-T],-N=-m\left[\frac{\partial u}{\partial y}\right],D_m\left[\frac{\partial C}{\partial y}\right]=h_2[C_w-C],\ \text{as}\ y\to 0$$

$$u\to 0,T\to T_\infty,C\to C_\infty\quad\text{as}\ y\to\infty-----(7)$$

The stream function $\psi = \psi(x, y)$ for that given as

$$u = \frac{\partial \psi}{\partial y}, v = -\frac{\partial \psi}{\partial x}$$

Equations (1)-(4) are reformed into ordinary equations

$$\eta = \sqrt{\frac{a}{v}}y \text{ ---------------(8)}$$

The velocity components are

$$\varphi = \sqrt{av}\, xf(\eta), u = \frac{\partial \varphi}{\partial y} = axf'(\eta),\ N = ax\left(\sqrt{\frac{a}{v}}\right)h(\eta),$$

$$v = -\frac{\partial \varphi}{\partial x} = \sqrt{avf(\eta)}, \theta(\eta) = \frac{T - T_\infty}{T_w - T_\infty},\ \emptyset(\eta) = \frac{C - C_\infty}{C_w - C_\infty},$$

$$T = T_\infty(1 + (\theta_w - 1)\theta) \text{ --------------(9)}$$

Using Equation of (8) and (9) the governing Equations (2)–(4) are transformedas

$$\left[1 + \frac{1}{\beta}\right]f''' + ff' - (f')^2 + Kh' + (Gr_T\theta + Gr_c\varphi)\cos\alpha - Mf' = 0 - - - (10)$$

$$\left[1 + \frac{K}{2}\right]h'' + fh' - f'h - K\left[1 + \frac{1}{\beta}\right](2h + f'') = 0 - - - (11)$$

$$[1 + N_r\{1 + 3(\theta_w - 1) + 3(\theta_w - 1)^2\theta^2 + (\theta_w - 1)^3\theta^3\}]\theta''$$
$$+N_r[(\theta_w - 1)(\theta')^2 + 6(\theta_w - 1)^2\theta(\theta')^2$$
$$+3(\theta_w - 1)^3\theta^2(\theta')^2] + P_r f\theta' - P_r f'\theta + A^* f' + B^*$$
$$\theta + P_r Du\varphi'' + P_r E_c(f'')^2 = 0 - - - (12)$$

$$\phi'' + Scf\phi' - k_r Sc\phi + ScSr\theta'' = 0 - - - - (13)$$

here

$$Gr_T = \frac{g\beta_T(T_w - T_\infty)}{a^2 x}, N_r = \frac{16\sigma^* T_\infty^3}{3kk^*},\ Gr_C = \frac{g\beta_C(C_w - C_\infty)}{a^2 x}, Pr = \frac{\upsilon\rho C_p}{k} = \frac{\mu C_p}{k}, M = \frac{\sigma B_0^2}{a\rho},$$

$$\mathrm{Sr} = \frac{D_m K_T}{\upsilon T_m}\left(\frac{T_w - T_\infty}{C_w - C_\infty}\right), \mathrm{Sc} = \frac{\upsilon}{D_m}, \mathrm{Du} = \frac{D_m K_T(C_w - C_\infty)}{C_s C_p \upsilon(T_w - T_\infty)}, E_c = \frac{u^2}{C_p(T_w - T_\infty)}$$

$$K_r = \frac{k^*}{a} \text{ ----------(14)}$$

The transformed boundary settings are as follows,

$$f' = 1 + \gamma f'',\ f = 0,\ \theta' = Bi_T(1 - \theta),\ \emptyset' = Bi_c(1 - \emptyset) \text{ as } \eta \to 0,$$
$$f'(\eta) = 0,\ \theta(\eta) = 0,\ \emptyset(\eta) = 0 \text{ as } \eta \to \infty \text{ ---------(15)}$$

It is discovered that the nanofluid model lacks micropolar effects when vertex viscosity or $K = 0$ is eliminated. The Sherwood coefficient, the Nusselt, and friction coefficient are all defined by

$$C_{f_x} Re_x^{\frac{1}{2}} = \left(1 + \frac{1}{\beta}\right)f''(0) \text{ ----------(16)}$$

$$NuRe_x^{\frac{1}{2}} = -(1 + N_r(\theta_w)^3)\theta'(0) \text{--------(17)}$$

$$Sh\, Re_x^{-\frac{1}{2}} = -\emptyset'(0) \text{-----------}(18)$$

Here, $Re_x = \frac{xu_w}{\upsilon}$ signifies the Reynolds Number.

3. Fuzzification

Fuzzification is a process used in fuzzy logic to convert a crisp mathematical equation into a fuzzy form. This involves introducing fuzzy variables and parameters to account for uncertainty and imprecision. The given system of differential equations and apply fuzzy membership functions, we need to define fuzzy sets and membership functions for the parameters and variables. Define membership functions for the key parameters and variables. We'll use triangular membership functions for simplicity. Convert the crisp values of the parameters and variables into their fuzzy counterparts. For instance, if β=1.2, it might be represented as

- $\mu\beta L(1.2) = 0$
- $\mu\beta M(1.2) = 0.6$
- $\mu\beta H(1.2) = 0.4$

Establish rules to relate input fuzzy sets to output fuzzy sets. For example, if β is Low and K is Medium, then f' is High. If GrT is High and θ is Medium, then θ'' is Low. Convert the fuzzy output sets back to crisp values using methods like the centroid method. For instance, If the output fuzzy set for f' has membership values 0.6 for Medium and 0.4 for High, the defuzzied value might be calculated as

$$f' = \frac{0.6 * 1 + 0.4 * 1.5}{0.6 + 0.4} = \frac{0.6 + 0.6}{1} = 1.2$$

This transformation incorporates uncertainties and imprecision into the system of equations. Let's convert the given system of equations into a fuzzified form

$$\left[1 + \frac{1}{\beta}\right]\tilde{f}''' + \tilde{f}\tilde{f}' - (\tilde{f}')^2 + K\widetilde{h}' + (G\widetilde{r_T}\tilde{\theta} + G\widetilde{r_c}\tilde{\varphi})\cos\tilde{\alpha} - \widetilde{M}\tilde{f}' = 0 --- (19)$$

$$\left[1 + \frac{K}{2}\right]\widetilde{h}'' + f\tilde{h}' - \tilde{f}'\tilde{h} - K\left[1 + \frac{1}{\beta}\right](2\tilde{h} + \tilde{f}'') = 0 --- (20)$$

$$\begin{aligned}
&[1 + N_r\{1 + 3(\widetilde{\theta_w} - 1) + 3(\widetilde{\theta_w} - 1)^2\tilde{\theta}^2 + (\widetilde{\theta_w} - 1)^3\widetilde{\theta^3}\}]\tilde{\theta}'' \\
&+N_r[(\widetilde{\theta_w} - 1)(\tilde{\theta}')^2 + 6(\tilde{\theta}_w - 1)^2\tilde{\theta}(\tilde{\theta}')^2 \\
&+3(\tilde{\theta}_w - 1)^3\tilde{\theta}^2(\tilde{\theta}')^2] + P_r\tilde{f}\tilde{\theta}' - P_r\tilde{f}'\tilde{\theta} + A^*\tilde{f}' \\
&+B^*\tilde{\theta} + P_r Du\tilde{\varphi}'' + P_r E_c\left(\tilde{f}''\right)^2 = 0 --- (21)
\end{aligned}$$

$$\tilde{\varphi}'' + Sc\tilde{f}\tilde{\varphi}' - k_r Sc\tilde{\varphi} + ScSr\widetilde{\theta}'' = 0 ---- (22)$$

Table 1: Comparison values of $-\theta'(0)$ and $-\varphi'(0)$ with the results of Hayat [11].

β	Hayat [11]		Present results	
	$-\theta'(0)$	$-\varphi'(0)$	$\theta'(0)$	$-\varphi'(0)$
0.8	0.65027	0.71096	0.65035	0.71341
1.4	0.62182	0.68252	0.62178	0.68015
3	0.59241	0.63305	0.59239	0.64610

4. Results and discussion

The nonlinear equations (10) – (15) are solved numerically by MATLAB bvp4c method. For graphical results, we considered $\beta = 1.5, Gr_T = 0.8, M = 1.5$, $Nr = 0.2$, $A^* = B^* = 0.1$, $Pr = 7$, $\theta_w = 2$, $Gr_c = 0.8$, $BiT = 2$, $BiC = 2$, $Sc = 0.6$, $Kr = 0.2$, $Sr = 0.2$, $Ec = 0.2$ and Du = 0.1 . The plots, $f'(\eta), \theta(\eta)$ and $\phi(\eta)$ indicate the corresponding flow fields' curves. Figs 2-5 displays Effects of the magnetic terms on the velocity plot, temperature and concentration and micropolar. As soon as the M value's is raised, a velocity reduction is seen. When applied transversely in the flow direction, M will create the Lorentz force due to its strong force on fluid flow. Lorentz force in electromagnetism has applications in hydrodynamics, plasma accelerators, MHD accelerators, and other engineering fields. An electrically conductive liquid's flow is slowed by the Lorentz force. As a result, the Lorentz force causes the velocity and momentum boundary layer thickness to decrease as soon as the magnetic parameter increases. The temperature and concentration increase when magnetic parameter is grown. As a result, force will be formed on the nanofluid flow then received some heat energy. When M increased then micropolar also raised. Figs 6-9 depict casson parameter on the flow environs such as Velocity Profile, temperature, concentration and micro rotation. Velocity profile and microrotation declined for larger β while $\theta, \emptyset$ are embellished for the raise β. Fig 10-17 depicts the Dufour and soret factor on the flow fields. The applied magnetic field tends to impede fluid motion and decrease the velocity profile, θ and microrotation as Du increases. Dufour and soret opposite reaction in temperature and concentration. Fig 18-21 shows the fallout of the Eckert thing on the concentration boost remain reduce. The calefaction grows as Eckert number raise and concentration slightly increase with increasing Eckert number. Fig 22-25 shows the fallout of the Prandtl thing on the concentration delineation remain boost. The calefaction grows as Prandtl number decrease and concentration slightly raise with increasing Prandtl number. Table 1 express good agreement with previous work [11]. Table 2 shows Sc and Nr in Nuand Sh. Increasing Schmidth Nusselt boost and Sherwood fall off. The chemical radiation parameter rise in both Nu and Sh. Table 3 express diverse values of physical confines on Cfx, Nu andSh. The Magnetic and Prandtl drop and others reversed in Cfx. Dufour and magnetic diminish others surge in Nu. Finally, the Sherwood quantity shows Eckert and dufour grows remain fall down.

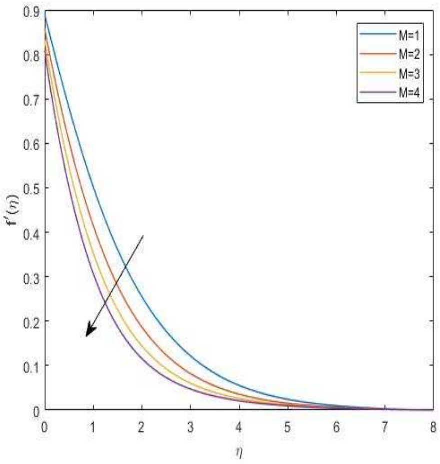

Fig 2: Magnetic field on $f'(\eta)$

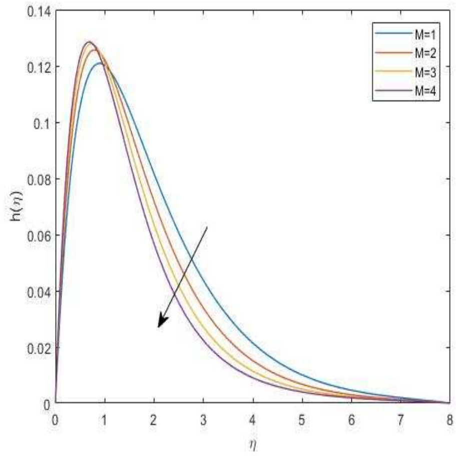

Fig 3: Magnetic field on $h(\eta)$

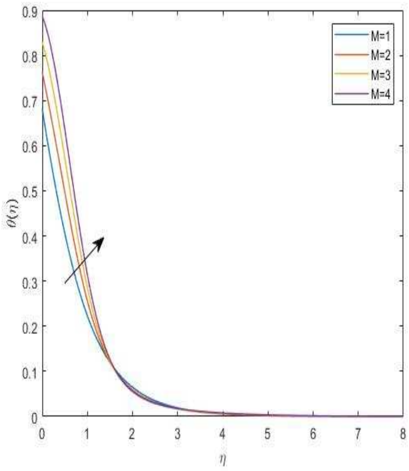

:

Fig 4: Magnetic field on $\theta(\eta)$

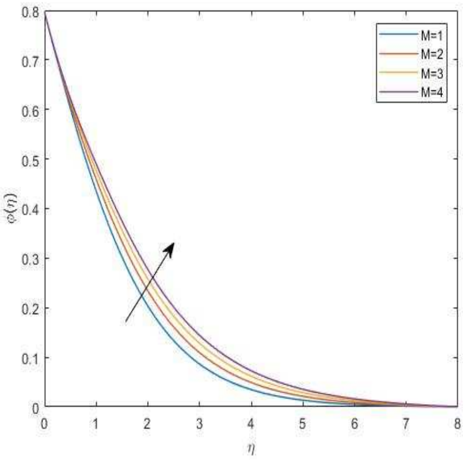

Fig 5: Magnetic field on $\varphi(\eta)$

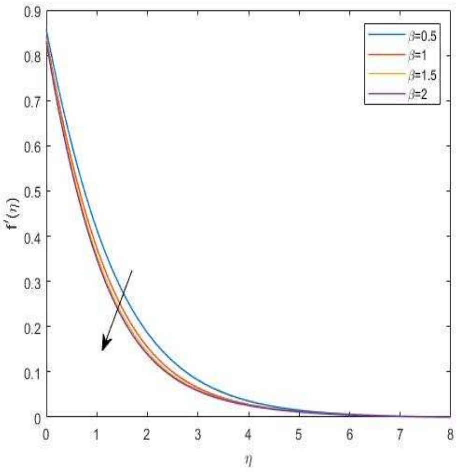

Fig 6: Casson parameter on $f'(\eta$

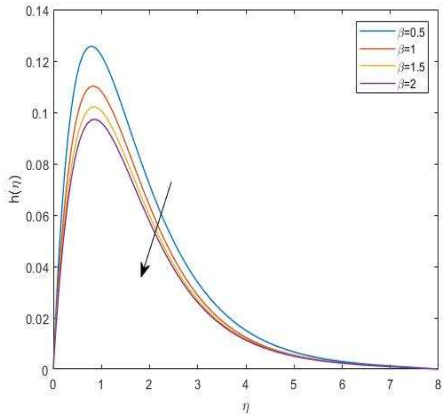

Fig 7: Casson parameter on $h(\eta)$

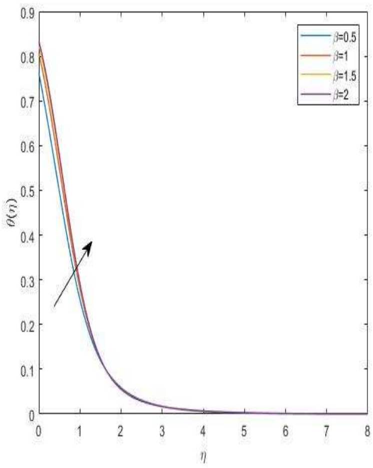

Fig 8: Casson parameter on $\theta(\eta)$

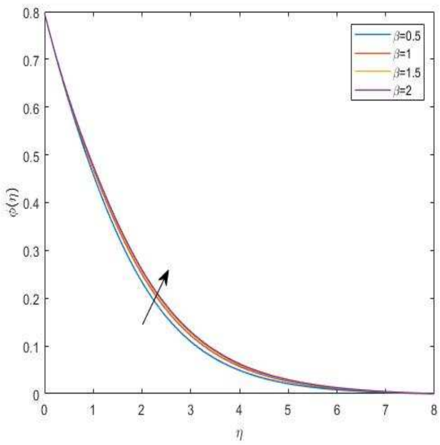

Fig 9: Casson parameter on $\varphi(\eta)$

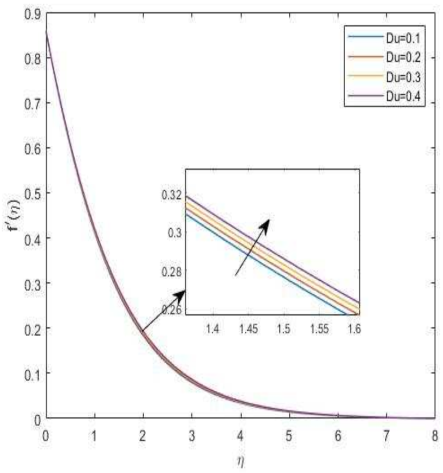

Fig 10: Dufour on $f'(\eta)$

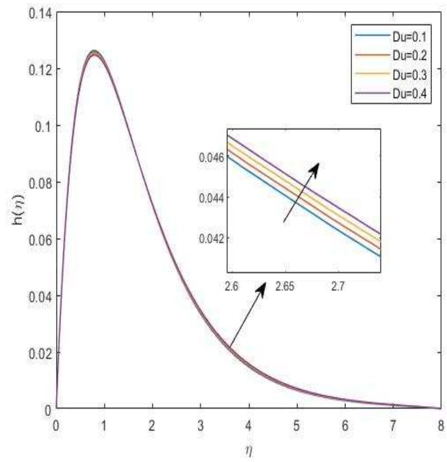

Fig 11: Dufour on $h(\eta)$

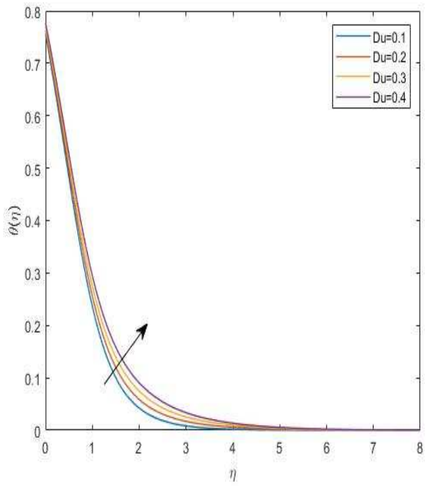

Fig 12: Dufour on $\theta(\eta)$

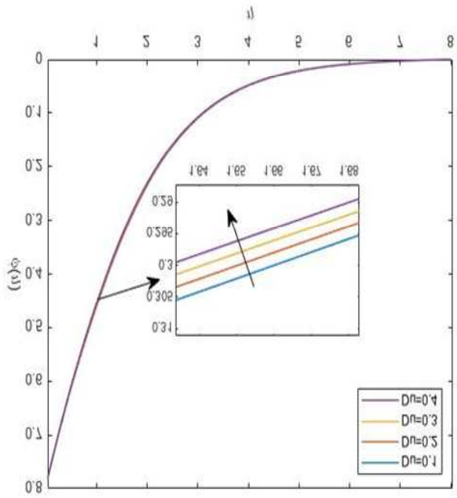

Fig 13: Dufour on $\varphi(\eta)$

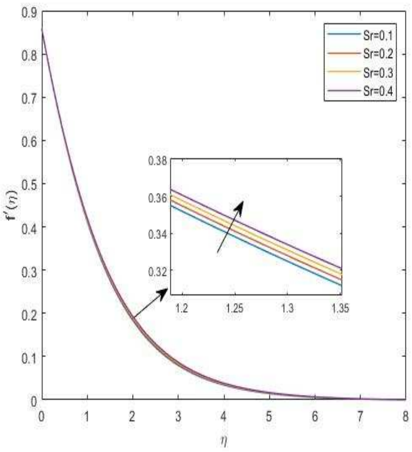

Fig 14: Soret on $f'(\eta)$

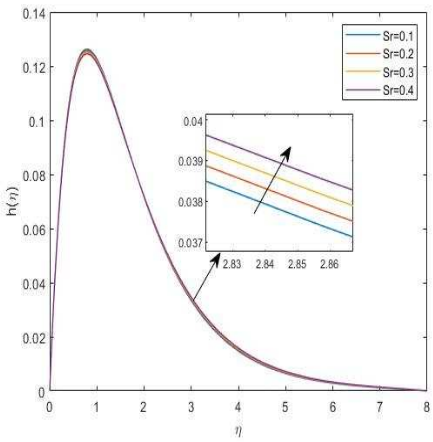

Fig 15: Soret on $h(\eta)$

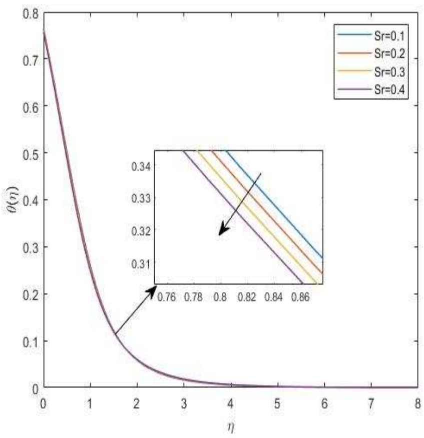

Fig 16: Soret on $\theta(\eta)$

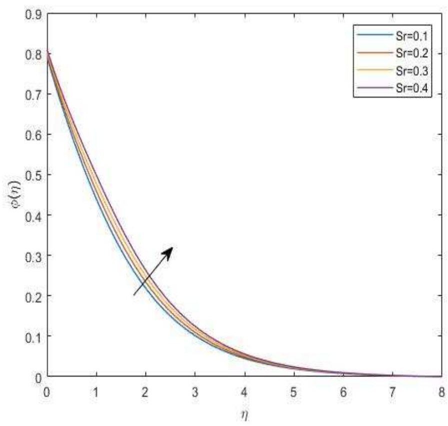

Fig 17: Soret on $\varphi(\eta)$

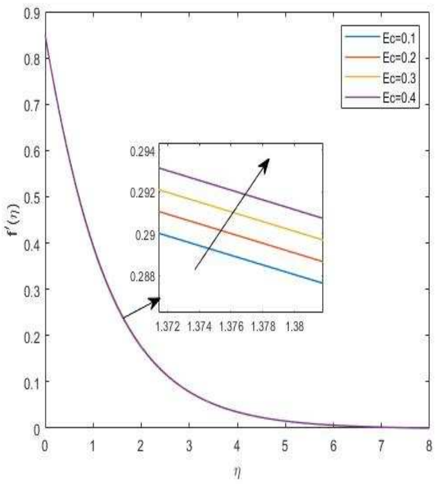

Fig 18: Eckert on $f'(\eta)$

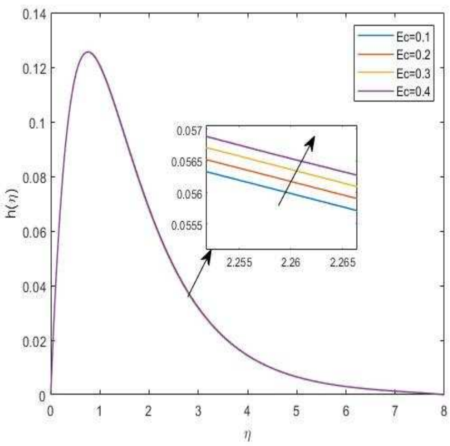

Fig 19: Eckert on $h(\eta)$

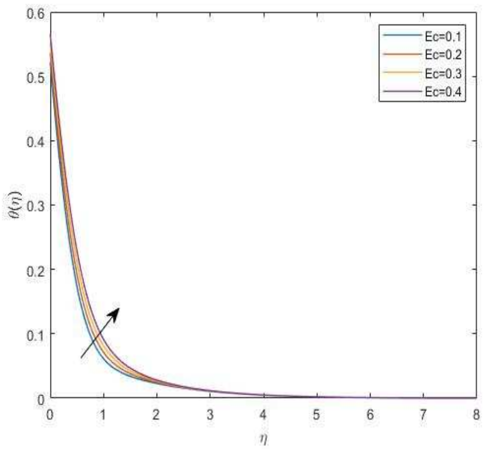

Fig 20: Eckert on $\theta(\eta)$

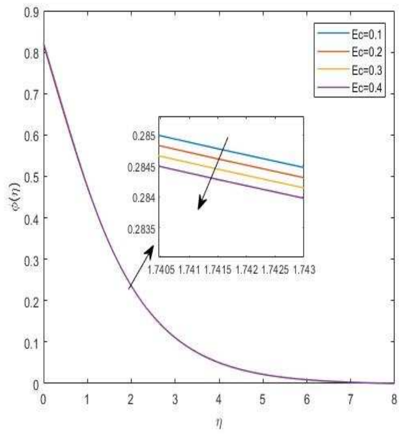

Fig 21: Eckert on $\varphi(\eta)$

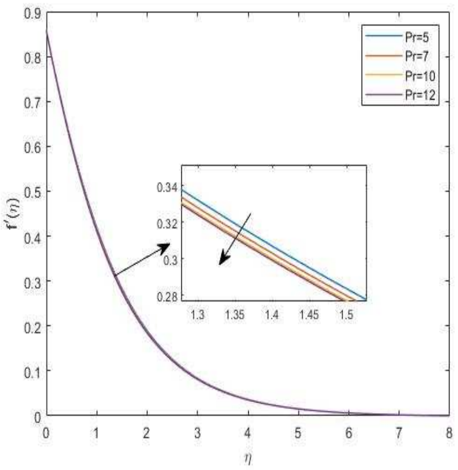

Fig 22: Prandlt on $f'(\eta)$

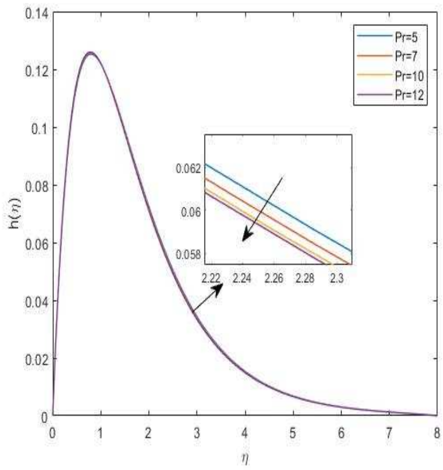

Fig 23: Prandlt on $h(\eta)$

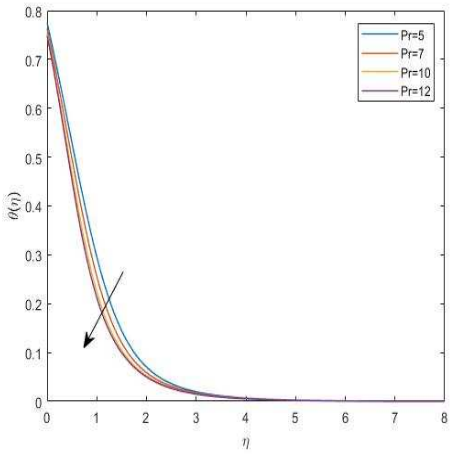

Fig 24: Prandlt on $\theta(\eta)$

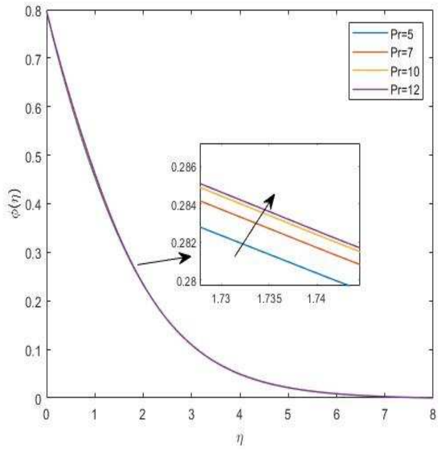

Fig 25: Prandlt on $\varphi(\eta)$

Table 2: Distinctive values of Sc and Nr in Nu and Sh

Sc	Nr	Nu	Sh
0.1		2.5199	0.1704
0.2		2.5115	0.2141
0.3		2.4995	0.2821
0.4		2.4910	0.3327
	0.1	1.8730	0.3239
	0.2	2.4910	0.3327
	0.3	3.0128	0.3402
	0.4	3.4598	0.3466

Table 3: Values of $Cfx, Nu\ and\ Sh$

M	Pr	Du	Sr	Ec	C_{fx}	Nu	Sh
1.0					-1.3204	1.6573	0.4080
2.0					-1.7118	1.2357	0.4067
3.0					-2.0266	0.8858	0.4070
4.0					-2.2915	0.5909	0.4082
	5				-1.6981	1.1692	0.4094
	7				-1.7118	1.2357	0.4067
	10				-1.7230	1.2891	0.4045
	12				-1.7276	1.3096	0.4037
		0.1			-1.7199	1.2732	0.4050
		0.2			-1.7118	1.2357	0.4067
		0.3			-1.7038	1.1979	0.4084
		0.4			-1.6958	1.1598	0.4101
			0.1		-1.7184	1.2214	0.4187
			0.2		-1.7118	1.2357	0.4067
			0.3		-1.7052	1.2502	0.3942
			0.4		-1.6984	1.2647	0.3812
				0.1	-1.8293	2.4884	0.3542
				0.2	-1.8226	2.4102	0.3575
				0.3	-1.8159	2.3336	0.3608
				0.4	-1.8093	2.2586	0.3639

5. Conclusion

Eckert number with the presence of chemical reaction on Casson micropolar nanofluid flow over an inclined Magnetic field are analyzed. The findings might be beneficial in subsequent innovations utilizing stretchy material-based aqueous platforms.

The major findings are

- While the humidity and concentration gradients progress, the velocity hinders as the Casson index and M mature.
- The Soret quantity Sr has counterproductive consequence for $\theta(\eta)$ and $\phi(\eta)$
- The ambient temperature drops as Pr increases, and the depth of the warmth barrier lowers as Prandtl grows.

- Eckert growth in velocity and angular momentum reversed in $\theta(\eta)$ and $\phi(\eta)$. Nusselt, Sherwood and skin friction improved in the enlarge value of Eckert.

Casson micropolar nanofluids, which possess improved heat transfer characteristics and the capability to react to magnetic fields, have potential applications in hyperthermia therapy. Employing fuzzy logic-based control systems could enhance the precision of thermal energy delivery to cancerous tissues, thereby optimizing therapeutic outcomes while reducing harm to healthy tissues. Future research should explore the possible synergies by combining Casson micropolar nanofluids with other cancer treatment methods, such as immunotherapy or photodynamic therapy. Integrate optimization algorithms alongside fuzzy logic to improve the effectiveness of systems utilising Casson micropolar nanofluids. Investigate incorporating fuzzy logic-based control systems to monitor and optimize thermal processes in real-time using Casson micropolar nanofluids.

Acknowledgement. We would like to provide our cordial thanks to the honourable referees for their valuable comments which helped us enrich the paper's quality.

Conflict of interest. There is no conflict no conflict of interest among the authors.

Authors' Contributions. All authors contributed equality.

REFERENCES

1. T. Abbas, M. M. Bhatti and M. Ayub, Aiding and opposing of mixed convection Casson nanofluid flow with chemical reactions through a porous Riga plate, *Proc. Inst. Mech. Eng. Part E J. Process. Mech. Eng.*, 232 (2018) 519-527.
2. S. Z. Abbas, M. Waqas, A. Thaljaoui, et al., Modeling and analysis of unsteady second-grade nanofluid flow subject to mixed convection and thermal radiation, *Soft Comput.*, 26 (2022) 1033-1042.
[Online]. Available: https://doi.org/10.1007/s00500-021-06575-7
3. W. Adnan, N. M. Said, et al., Significance of coupled effects of resistive heating and perpendicular magnetic field on heat transfer process of mixed convective flow of ternary nanofluid, *J. Therm. Anal. Calorim.*, 2023.
[Online]. Available: https://doi.org/10.1007/s10973-023-12723-y
4. K. Afzal and A. Aziz, Transport and heat transfer of time dependent MHD slip flow of nanofluids in solar collectors with variable thermal conductivity and thermal radiation, *Results Phys.*, 6 (2016) 746-753.
5. H. Alotaibi, S. Althubiti, M. R. Eid and K. L. Mahny, Numerical treatment of MHD flow of Casson nanofluid via convectively heated non-linear extending surface with viscous dissipation and suction/injection effects, *Comput. Mater. Continua*, 66(1) (2021) 229-245.
6. K. Anantha, V. Sugunamma and N. Sandeep, Influence of viscous dissipation on MHD flow of micropolar fluid over a slendering stretching surface with modified heat flux model, *J. Therm. Anal. Calorim.*, 139(4) (2019) 3661-3674.
[Online]. Available: https://doi.org/10.1007/s10973-019-08694-8

7. T. Anusha, U. S. Mahabaleshwar and Y. Sheikhnejad, An MHD of nanofluid flow over a porous stretching/shrinking plate with mass transpiration and Brinkman ratio, *Transp. Porous Med.*, 142 (2022) 333-352.
[Online]. Available: https://doi.org/10.1007/s11242-021-01695-y
8. M. Deivanayaki, M. Jannath Begam, A. Henna Shenofer and B. Arun, Free convection of Casson nanofluid with inclined magnetic field, *AIP Conf. Proc.*, 2327(1) (2021) 020057. [Online]. Available: http://dx.doi.org/10.1063/5.0039436
9. S. Ghasemi and M. Hatami, Solar radiation effects on MHD stagnation point flow and heat transfer of a nanofluid over a stretching sheet, *Case Stud. Therm. Eng.*, 25 (2021) 100898.
10. D. Gopal, N. Kishan and C. Raju, Viscous and Joule's dissipation on Casson fluid over a chemically reacting stretching sheet with inclined magnetic field and multiple slips, *Inform. Med. Unlocked*, 9 (2017) 154-160.
11. T. Hayat, S. A. Shehzad and A. Alsaedi, Soret and Dufour effects on magnetohydrodynamic (MHD) flow of Casson fluid, *Appl. Math. Mech. (Engl. Ed.)*, 33(10) (2012) 1301-1312.
[Online]. Available: https://doi.org/10.1007/s10483-012-1623-6
12. A. Hamid, M. Khan and A. S. Alshomrani, Non-linear radiation and chemical reaction effects on slip flow of Williamson nanofluid due to a static/moving wedge: a revised model, *Appl. Nanosci.*, 10 (2020) 3171-3181.
[Online]. Available: https://doi.org/10.1007/s13204-019-01172-5
13. S. Jain and R. Kumari, Analysis of Casson nanofluid flow and heat transfer across a non-linear stretching sheet adopting Keller box finite difference scheme, *Int. J. Appl. Comput. Math.*, 9 (2023) 134.
[Online]. Available: https://doi.org/10.1007/s40819-023-01619-y
14. W. Jamshed, M. Goodarzi, M. Prakash, K. S. Nisar, M. Zakarya, A.-H. Abdel-Aty, et al., Evaluating the unsteady Casson nanofluid over a stretching sheet with solar thermal radiation: an optimal case study, *Case Stud. Therm. Eng.*, 26 (2021) 101160.
15. M. Jannath Begam, M. Deivanayaki, B. Arun and A. Henna Shenofer, Casson fluid flow past a porous medium with heat source in the presence of an inclined magnetic field, *AIP Conf. Proc.*, 2327 (2021) 020058.
16. A. Kumar, R. Tripathi and R. Singh, Entropy generation and regression analysis on stagnation point flow of Casson nanofluid with Arrhenius activation energy, *J. Braz. Soc. Mech. Sci. Eng.*, 41 (2019) 306.
[Online]. Available: https://doi.org/10.1007/s40430-019-1803-y
17. P. V. Kumar, Ch. Sunitha, G. Lorenzini and S. M. Ibrahim, A study of thermally radiant Williamson nanofluid over an exponentially elongating sheet with chemical reaction via homotopy analysis method, *CFD Lett.*, 14(5) (2022) 68-86.
18. P. V. Kumar, C. Sunitha, S. M. Ibrahim, et al., Outlining the slip effects on MHD Casson nanofluid flow over a permeable stretching sheet in the existence of variable wall thickness, *J. Eng. Thermophys.*, 32 (2023) 69-88.
[Online]. Available: https://doi.org/10.1134/S1810232823010071
19. U. S. Mahabaleshwar, T. Anusha and M. Hatami, The MHD Newtonian hybrid nanofluid flow and mass transfer analysis due to super-linear stretching sheet embedded in porous medium, *Sci. Rep.*, 11 (2021) 22518.
[Online]. Available: https://doi.org/10.1038/s41598-021-01902-2

20. S. Naramgari and C. Sulochana, Dual solutions of radiative MHD nanofluid flow over an exponentially stretching sheet with heat generation/absorption, *Appl. Nanosci.*, 6 (2016) 131-139.
[Online]. Available: https://doi.org/10.1007/s13204-015-0420-z
21. M. K. Nayak, S. Shaw, V. S. Pandey, et al., Combined effects of slip and convective boundary condition on MHD 3D stretched flow of nanofluid through porous media inspired by non-linear thermal radiation, *Indian J. Phys.*, 92 (2018) 1017-1028.
[Online]. Available: https://doi.org/10.1007/s12648-018-1188-2
22. D. Pal and N. Roy, Lie group transformation on MHD double-diffusion convection of a Casson nanofluid over a vertical stretching/shrinking surface with thermal radiation and chemical reaction, *Int. J. Appl. Comput. Math.*, 4 (2018) 13. [Online]. Available: https://doi.org/10.1007/s40819-017-0449-7
23. K. Rafique, M. I. Anwar and M. Misiran, Numerical study on micropolar nanofluid flow over an inclined surface by means of Keller-Box, *Asian J. Probab. Stat.*, 1 (2019) 1–21.
24. G. Rasool, A. Shafiq, M. S. Alqarni, A. Wakif, I. Khan and M. S. Bhutta, Numerical scrutinization of Darcy-Forchheimer relation in convective magnetohydrodynamic nanofluid flow bounded by nonlinear stretching surface in the perspective of heat and mass transfer, *Micromachines*, 12(4) (2021) 374.
doi: 10.3390/mi12040374.
25. M. B. Shaheen, K. S. Arain, A. Nisar, M. D. Albakri, F. O. Shamshuddin and U. Mallawi, A case study of heat transmission in a Williamson fluid flow through a ciliated porous channel: a semi-numerical approach, *Case Studies in Thermal Engineering*, 41 (2023) 102523. doi: 10.1016/j.csite.2022.102523.
26. R. Sharma, S. M. Hussian, C. S. K. Raju, G. S. Seth and A. J. Chamkha, Study of graphene Maxwell nanofluid flow past a linearly stretched sheet: a numerical and statistical approach, *Chinese J. Phys.*, 68 (2020) 671–683.
27. G. C. Shit and S. Mandal, Entropy analysis on unsteady MHD flow of Casson nanofluid over a stretching vertical plate with thermal radiation effect, *Int. J. Appl. Comput. Math*, 6(2) (2020) 2. doi: 10.1007/s40819-019-0754-4.
28. K. Suneetha, S. M. Ibrahim, G. V. Ramana Reddy and P. Vijaya Kumar, Analytical study of induced magnetic field and heat source on chemically radiative MHD convective flow from a vertical surface, *J. Comput. Appl. Res. Mech. Eng.*, 11(1) (2021) 165–176.
29. H. S. Takhar, A. J. Chamkha and G. Nath, Flow and heat transfer on a stretching surface in a rotating fluid with a magnetic field, *Int. J. Therm. Sci.*, 42(1) (2003) 23–31.
30. T. Thumma, O. A. Beg and A. Kadir, Numerical study of heat source/sink effects on dissipative magnetic nanofluid flow from a non-linear inclined stretching/shrinking sheet, *J. Mol. Liq.*, 232 (2017) 159–173.
31. I. Ullah, I. Khan and S. Shafie, MHD natural convection flow of Casson nanofluid over nonlinearly stretching sheet through porous medium with chemical reaction and thermal radiation, *Nanoscale Res. Lett.*, 11 (2016) 527. doi: 10.1186/s11671-016-1745-6.
32. W. Jamshed, S. U. Devi, M. Goodarzi, M. Prakash, K. S. Nisar, M. Zakarya and A. A.-H. Abdel-Aty, Evaluating the unsteady Casson nanofluid over a stretching sheet with solar thermal radiation: An optimal case study, *Case Studies in Thermal Engineering*, 26 (2021) 101160. doi: 10.1016/j.csite.2021.101160.

33. M. Yaseen, S. K. Rawat, U. Khan, I. E. Sarris, H. Khan, A. S. Negi, A. Khan, E. S. M. Sherif, A. M. Hassan and A. Zaib, Numerical analysis of magnetohydrodynamics in an Eyring-Powell hybrid nanofluid flow on wall jet heat and mass transfer, *Nanotechnology*, 2023. doi: 10.1088/1361-6528/acf3f6.
34. L. Li, S. Kosari, S. H. Sadati and A. A. Talebi, Concepts of Vertex Regularity in Cubic Fuzzy Graph Structures with an Application, *Frontiers in Physics*, 10 (2022) 1324.
35. X. Shi, S. Kosari, H. Rashmanlou, S. Broumi and S. S. Hussain, Properties of interval-valued quadripartitioned neutrosophic graphs with real-life application, *Journal of Intelligent & Fuzzy Systems*, (2023)1-15.
36. X. Qiang, M. Akhoundi, Z. Kou, X. Liu and S. Kosari, Novel Concepts of Domination in Vague Graphs with Application in Medicine, *Mathematical Problems in Engineering*, 202 (2021).
37. M. Shoaib, S. Kosari, H. Rashmanlou, M. A. Malik, Y. Rao, Y. Talebi and F. Mofidnakhaei, Notion of Complex Pythagorean Fuzzy Graph with Properties and Application, *Journal of Multiple-Valued Logic & Soft Computing*, 34 (2020).
38. X. Shi, S. Kosari, A. A. Talebi, S. H. Sadati and H. Rashmanlou, Investigation of the main energies of picture fuzzy graph and its applications, *International Journal of Computational Intelligence Systems*, 15(1) (2022) 31.
39. Y. Rao, R. Chen, P. Wu, H. Jiang and S. Kosari, A Survey on Domination in Vague Graphs with Application in Transferring Cancer Patients between Countries, *Mathematics*, 9(11) (2021) 1258.
40. S. Kosari, Z. Shao, Y. Rao, X. Liu, R. Cai and H. Rashmanlou, Some Types of Domination in Vague Graphs with Application in Medicine, *Journal of Multiple-Valued Logic & Soft Computing*, 41 (2023).
41. Y. Rao, S. Kosari, J. Anitha, I. Rajasingh and H. Rashmanlou, Forcing parameters in fully connected cubic networks, *Mathematics*, 10(8) (2022) 1263.
42. S. Samanta, M. Pal, H. Rashmanlou and R. A. Borzooei, Vague graphs and strengths, *Journal of Intelligent & Fuzzy Systems*, 30(6) 2016) 3675-3680.
43. R. A. Borzooei and H. Rashmanlou, Cayley interval-valued fuzzy graphs, *UPB Scientific Bulletin, Series A: Applied Mathematics and Physics*, 78(3) (2016) 83-94.
44. Z. Shao, Y. Rao, S. Kosari, H. Rashmanlou and F. Mofidnakhaei, Certain Notions of Regularity in Vague Graphs With Novel Application, *Journal of Multiple-Valued Logic & Soft Computing*, 40 (2023).
45. S. Kosari, H. Jiang, A. Khan and M. Akhoundi, Properties of Connectivity in Vague Fuzzy Graphs With Application in Building University, *Journal of Multiple-Valued Logic & Soft Computing*, 41(6) (2023).
46. N. Ramya and M. Deivanayaki, Numerical Simulation of Casson Micropolar Fluid Flow Over an Inclined Surface Through Porous Medium, *Journal of Mines, Metals and Fuels*, 71(11) (2023) 2143-2149.
doi: 10.18311/jmmf/2023/36269.